Inertial dynamics of pinned charge-density-wave condensates. II. Orthorhombic TaS_3

S. Sridhar, D. Reagor, and G. Gruner
Department of Physics and Solid State Science Center, University of California, Los Angeles, California 90024
(Received 28 October 1985)

Complex conductivity $\sigma_{CDW}(\omega,T)$ measurements in the ranges 10—110 GHz and 20—300 K are reported on the charge-density-wave (CDW) material orthorhombic TaS_3. In the CDW state between approximately 130 and 210 K, the complex conductivity obeys a Drude behavior $\sigma_{CDW}(\omega)=(ne^2\tau/m^*)(1+i\omega\tau)$, which we associate with damped inertial response of the CDW. The measurements, together with earlier results in the radio-frequency spectral range, enable us to extract all the phenomenological parameters: damping constant τ, effective mass m^*, pinning frequency ω_0, and maximum CDW conductivity σ_{max}. The experimental results for these parameters are compared with available microscopic theories. The full dynamic response of the CDW between 10^7 and 10^{11} Hz is also presented and shows the conductivity resonance well below the single-particle gap, representing both the relaxational and inertial dynamic response of the collective CDW mode. A comparison is made to similar results on the related CDW compound $NbSe_3$.

I. INTRODUCTION

Orthorhombic TaS_3 (o-TaS_3) is a quasi-one-dimensional inorganic conductor in which the electronic ground state is well established to correspond to a charge-density wave (CDW) (Ref. 1) below a Peierls transition temperature $T_P\simeq 225$ K. In the CDW state, the material displays strikingly novel transport properties,[2] such as nonlinear and strongly frequency-dependent conductivity, narrow band noise, etc. qualitatively similar to those observed in $NbSe_3$. These have been interpreted as due to the collective response of the electrons condensed in the CDW state. In an accompanying paper[3] (hereafter called I), the frequency-dependent conductivity, measured in the microwave and millimeter-wave spectral range is discussed in terms of the collective response of the pinned CDW mode in the inorganic compound $NbSe_3$. Here we present experimental results in related compound of the same family, o-TaS_3.

The single-particle band is more anisotropic in o-TaS_3 than in $NbSe_3$. Consequently, The Peierls transition opens up a gap at the whole Fermi surface, leading to a semiconducting behavior below the transition. The gradual freezing out of the normal electrons with decreasing temperature is expected to have important consequences. While the normal electrons in $NbSe_3$ can, in principle, contribute both to the screening of long-wavelength fluctuations, and also to damping, such effects are unimportant in o-TaS_3, at least well below the Peierls transition. Another difference between the two materials is that o-TaS_3 becomes commensurate with the underlying lattice as the temperature is lowered[4] (with a CDW period, λ, of 4 times the lattice constant), while in $NbSe_3$, in both phases, λ is incommensurate with the lattice period.

In this paper we report extensive measurements of the complex conductivity $\sigma_{CDW}(\omega)$ of o-Tas_3 between 10 and 100 GHz and as a function of temperature. Between 210 K and approximately 130 K in the CDW state, our results for $\sigma_{CDW}(\omega)$ can be very well described by the Drude law:[5]

$$\sigma_{CDW}(\omega)=\sigma_{max}\frac{1}{1+i\omega\tau}=\frac{ne^2\tau}{m^*}\frac{1}{1+i\omega\tau}\ , \tag{1}$$

where m^* is the effective mass, n is the number of condensed electrons, and τ is the damping constant.

Thus the response of the CDW in the present spectral range can be described in terms of a damped inertial dynamics of the CDW. From the data the CDW parameters σ_{max}, the maximum CDW contribution to the conductivity and τ, the damping constant can be directly extracted. Further, since $\sigma_{max}=ne^2\tau/m^*$, the effective mass m^* of the CDW condensate is obtained.

Below 10 GHz, extensive available measurements of $\sigma_{CDW}(\omega)$ reveal that at these lower frequencies, the CDW response is relaxational.[6—8] In contrast, at higher frequencies used in this work, we observe inertial response. Combining all the available results below 100 GHz, we clearly show that the full dynamic response of the CDW is in the form of a collective conductivity mode. A simple description of this mode in a single oscillator model gives

$$\sigma_{CDW}(\omega)=\frac{ne^2\tau}{m^*}\frac{j\omega}{\tau(\omega_0^2-\omega^2)+j\omega}\ , \tag{2}$$

where ω_0 is a phenomenological pinning frequency. The low-frequency measurements yield a crossover frequency $\omega_{co}=\omega_0^2\tau$, which with the present measurements of τ yields ω_0. Thus we obtain all the phenomenological parameters, m^*, τ, and ω_0, associated with dynamics of the pinned CDW mode. Deviations from Eq. (2) at low frequencies have been extensively discussed in the literature.[7]

An analysis in terms of Eqs. (1) and (2) provides an adequate description of our experimental results at temperatures below 210 and 100 K, and effects associated with disorder provided by randomly distributed impurity centers plays an important role only in the very-low-frequency end of the spectrum, at radio frequencies.[8] Below about 100 K, disorder effects become more prominent, leading to serious deviations from Eq. (2) even in the spectral range covered by this study.

II. EXPERIMENTAL METHODS AND RESULTS

Here we briefly provide several experimental details specific to TaS_3, and refer the reader to I and Ref. 9 for further details.

The TaS_3 samples were prepared using well-known techniques.[6] The Peierls transition temperature, evaluated from the temperature derivative of the dc resistivity dR/dT was found to be $T_P = 220 \pm 2$ K, and the threshold electric field for nonlinear conduction $E_T = 200$ mV/cm at $T = 150$ K. Consequently, our materials have a purity comparable to pure o-TaS_3 specimens used by various groups.[2] We also note that, while both E_T, and the low-frequency behavior of σ_{CDW} are sensitive to impurity concentration and other (uncontrolled) defects, at microwave and millimeter-wave frequencies our results depend only weakly on impurities.

Complex conductivity measurements at fixed frequencies 32, 60, 94, and 109 GHz were carried out utilizing mm-wave bridges, as discussed in Ref. 9. For the mm-wave bridge measurements, very thin (cross-sectional area $\sim 1\ \mu m^2$) needless of typical lengths 2–4 mm (exceeding the small waveguide dimension for a given band) were selected. In contrast to $NbSe_3$, the conductivity of TaS_3 is low at all temperatures. Consequently, the series geometric reactance of the sample (see I), which was inductive for all the samples due to their selected lengths, was small compared to the intrinsic impedance due to their conductivity. This enables us to extract both the real and imaginary parts of $\sigma(\omega)$.

The results reported here are independent of mm-wave power. They are reproducible for samples within the same batch and for samples of different batches. Our measurements at 9 GHz are consistent with previous measurements at the same frequency reported in the literature.[10]

The total conductivity $\mathrm{Re}\sigma(\omega,T)$ measured at dc and several microwave and millimeter-wave frequencies is shown in Fig. 1 as a function of temperature between 300 and 20 K. The data is normalized to the room-temperature dc value. The qualitative features of the data are as follows.

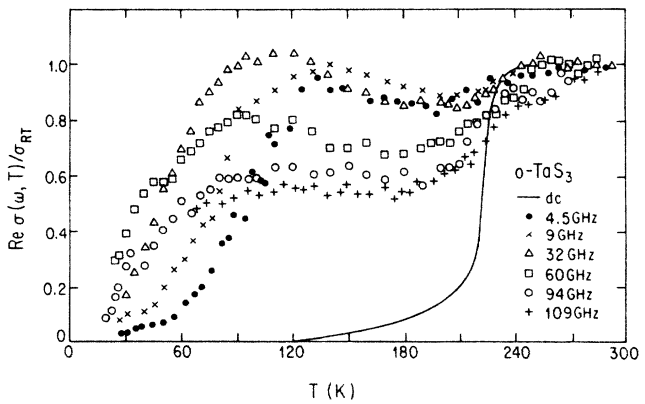

FIG. 1. Real part of the total conductivity $\mathrm{Re}\sigma(\omega,T)$ normalized to the room-temperature value σ_{RT} plotted as a function of temperature T for o-TaS_3, at dc, 9, 32, 94, and 109 GHz.

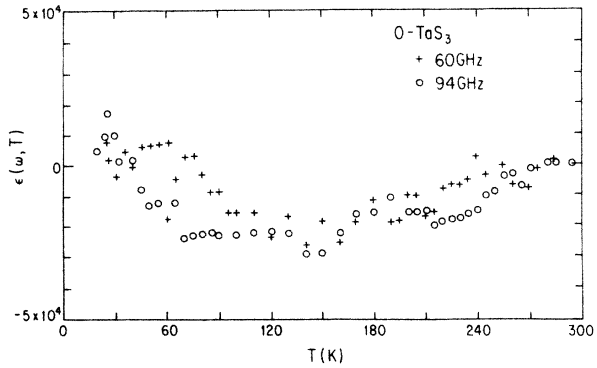

FIG. 2. Real part of the dielectric constant $\mathrm{Re}\epsilon(\omega,T)$ versus temperature at 60 and 94 GHz.

(1) Almost no frequency dependence is observed between 300 K and the transition temperature $T_P = 225$ K, consistent with metallic behavior in the normal state.

(2) Below T_P, in the CDW state, a strong frequency dependence develops. Between 210 K and approximately 100 K the conductivity is clearly decreasing with increasing frequency at frequencies above 10 GHz. Only a weak temperature dependence is observed in this temperature range.

(3) Below approximately 100 K, the ω dependence is much more complicated and is strongly temperature dependent.

The associated dielectric constant $\mathrm{Re}\epsilon(\omega,T)$ versus T measured at two frequencies, 60 and 94 GHz, is shown in Fig. 2. Above T_P, $\mathrm{Re}\epsilon$ is zero to within the measurement accuracy, again consistent with metallic behavior. In the CDW state below T_P, $\mathrm{Re}\epsilon$ is *negative* in the temperature region where $\mathrm{Re}\sigma$ is decreasing with ω. At low temperatures below ~ 100 K, $\mathrm{Re}\epsilon$ changes sign and becomes positive. (Similar data was obtained at 32 and 109 GHz but is not shown to avoid crowding.)

Figure 3, which is a plot of $\mathrm{Re}\sigma(\omega,T)$ versus $10^3/T$ at

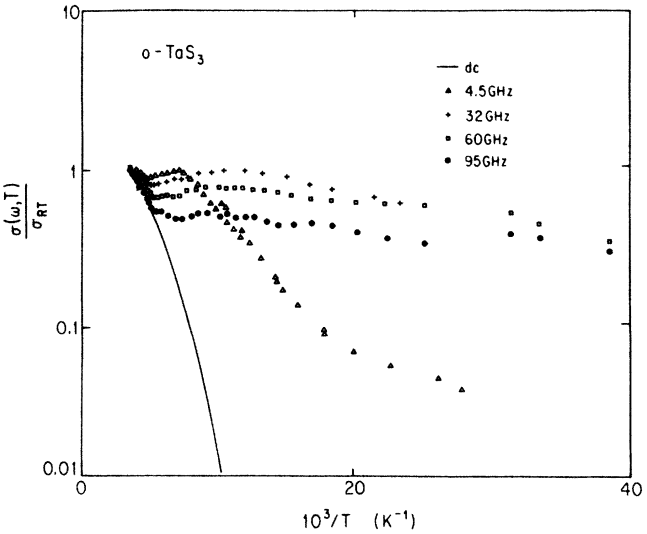

FIG. 3. $\mathrm{Re}\sigma(\omega,T)/\sigma_{RT}$ vs $10^3/T$ at dc, 9, 32, 60, and 94 GHz.

dc and high frequencies, clearly displays the magnitude of the effects being observed here. Below T_P, σ_{dc} decreases nearly exponentially with temperature due to the decreasing number of quasiparticles. However, the millimeter-wave conductivities are orders of magnitude higher, and show a much weaker T dependence. As our measuring frequencies are much smaller than the single-particle gap, consequently the extra conductivity at these high frequencies is to be associated with the electrons condensed in the CDW state.

III. ANALYSIS AND DISCUSSION

The frequency dependence of the CDW contribution to the conductivity

$$\mathrm{Re}\sigma_{\mathrm{CDW}}(\omega,T)=\mathrm{Re}\sigma(\omega,T)-\sigma_{\mathrm{dc}}(T)$$

and

$$\mathrm{Im}\sigma_{\mathrm{CDW}}(\omega,T)=\mathrm{Im}\sigma(\omega,T)\ ,$$

both normalized to $\sigma_{\mathrm{dc}}(300\ \mathrm{K})$, are shown in Figs. 4 and 5 at representative temperatures. Figures 4(a) and 5(a) are typical of the data for the temperature region $130<T<210$ K; Figs. 4(b) and 5(b) for $100<T<130$ K, and Fig. 4(c) for $T\leq 90$ K.

An extensive body of experimental data is available in TaS_3 in the "low-"frequency spectral range below 10 GHz.[6–8] The results possess two dominant qualitative features: (1) $\mathrm{Re}\sigma_{\mathrm{CDW}}(\omega)$ increases with frequency tending to saturate at about 5–10 GHz, (2) $\mathrm{Im}\sigma$ or $\mathrm{Re}\epsilon$ is positive. The data are conventionally analyzed in terms of a "relaxational" dynamic response of the CDW, with a characteristic frequency called the "crossover" frequency $\omega_{co}/2\pi\sim 10^7$–$10^8$ Hz. Here a description in terms of a single harmonic oscillator response, while reproducing the overall qualitative features, has to be supplemented by a distribution of relaxation times, or pinning frequencies.[8] Alternatively, $\mathrm{Re}\sigma_{\mathrm{CDW}}(\omega)$ in this spectral range is analyzed in terms of a tunneling model,[8] wherein a photon-assisted tunneling description leads to $\mathrm{Re}\sigma_{\mathrm{CDW}}(\omega)$ in good agreement with experimental findings. Note that these lower-frequency measurements would, in the linear horizontal frequency scale of Figs. 4 and 5, be confined to the vertical axis near zero frequency. They are not included both for reasons of clarity and because they are not necessary for the present analysis. (The full frequency dependence will be discussed later.)

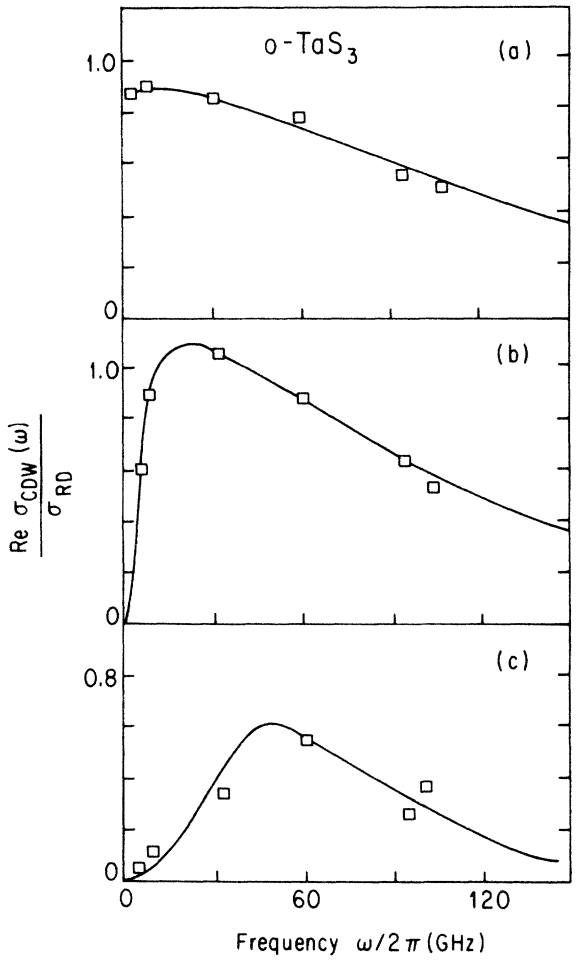

FIG. 4. $\mathrm{Re}\sigma_{\mathrm{CDW}}(\omega,T)$ normalized to the room-temperature conductivity σ_{RT} as a function of frequency $\omega/2\pi$ at (a) 160 K. The solid line is a fit of the data to the real part of Eq. (1) with $1/2\pi\tau=125$ GHz, $\sigma_{\max}=\mathrm{Re}\sigma_{\mathrm{CDW}}(9\ \mathrm{GHz})$. (b) Same as (a), but at 100 K. The solid line is a fit of the data to the real part of Eq. (2) using $1/2\pi\tau=100$ GHz, $\omega_0=21$ GHz. (c) Same as (a), but at 60 K. The solid line represents Eq. (2) with $1/2\pi\tau=80$ GHz, $\omega_0=55$ GHz.

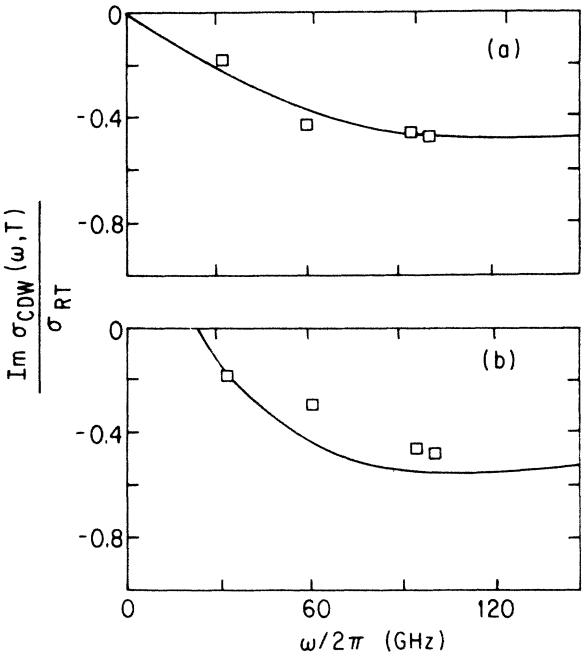

FIG. 5. $\mathrm{Im}\sigma_{\mathrm{CDW}}(\omega,T)$ normalized to σ_{RT} as function of $\omega/2\pi$ at (a) 160 K. The solid line is a fit to the imaginary part of Eq. (1) with the same parameters as in Fig. 4(a). (b) Same as (a), but at 100 K. The solid line is fit to the imaginary part of Eq. (2) with the same parameters as in Fig. 4(b).

Confining ourselves, for the moment, to the temperature range 210 to 130 K, the present data between 10 and 110 GHz possess two new qualitative features [see Figs. 4(a) and 5(a)].

(1) $\mathrm{Re}\sigma_{\mathrm{CDW}}(\omega)$ decreases with increasing frequency in the entire frequency range.

(2) $\mathrm{Im}\sigma_{\mathrm{CDW}}(\omega)$ and $\mathrm{Re}\epsilon(\omega)$ are negative in the full frequency range. We interpret these results in terms of a damped inertial response of the CDW, represented by the equation of motion

$$m^*\ddot{x}+\dot{x}/\tau=eE\exp(i\omega t)\ , \tag{3}$$

where x is the displacement of the CDW due to the driving electric field E. This yields the Drude behavior for σ_{CDW} given by Eq. (1). For the present temperature range (130–210 K), the data reveals that

$$\sigma_{\max}=ne^2\tau/m^*\simeq\mathrm{Re}\sigma_{\mathrm{CDW}}(9\ \mathrm{GHz})\ .$$

The solid lines in Figs. 4(a) and 5(a) are fits of the data to the real and imaginary parts of the Drude equation (1), from which the damping parameter $1/2\pi\tau$ is extracted. As Figs. 4(a) and 5(a) show, $\sigma_{\mathrm{CDW}}(\omega)$ is very well described by the damped inertial response represented by Eq. (1) with well-defined parameters. Furthermore, since $m^*=ne^2\tau/\sigma_{\max}$, the effective mass can also be calculated, with n being evaluated from the crystal structure and band filling. Thus three of the parameters of the CDW response: τ, m^*, and $\sigma_{\max}$ are obtained from the Drude response.

In the above analysis, pinning was ignored since the relaxational response occurs at these temperatures at much lower radio frequencies. However, the rf data can be combined with the present data to yield the pinning frequency ω_0. The single oscillator response Eq. (2) yields a characteristic frequency called the crossover frequency ω_{co}, which can be defined as the frequency at which $\mathrm{Im}\sigma$ reaches its maximum value (see Fig. 6). For TaS_3 at 160 K, this method gives $\omega_{\mathrm{co}}/2\pi=150$ MHz, which with $1/2\pi\tau=125$ GHz yields $\omega_0=4.3$ GHz. Since in practice the single oscillator response gives a semiquantitative but not accurate fit to the low-frequency data,[7] the evaluation of ω_{co} is not unambiguous. However, other methods of evaluating this quantity, e.g., as the frequency at which $\mathrm{Re}\sigma_{\mathrm{CDW}}(\omega_{\mathrm{co}})=\sigma_{\max}/2$, yield values which agree within a factor 2 with those evaluated from the frequency where $\mathrm{Im}\sigma(\omega)$ has a maximum.

Another method of evaluating ω_0 is by using the low-frequency dielectric constant together with the effective mass measured in this work, through the relation

$$\epsilon(\omega\rightarrow 0)=1+\frac{4\pi ne^2}{m^*\omega_0^2}\ . \tag{4}$$

At 160 K for TaS_3, ϵ(1 MHz) (Refs. 6 and 8) $=4\times10^7$ and $m^*/m_e=940$ from the present work. With $n=6.5\times10^{21}/\mathrm{cm}^3$ (Ref. 2), Eq. (4) yields $\omega_0/2\pi=3.7$ GHz, in agreement with the other method. It should also be noted that ω_0 is impurity and hence sample dependent.

In this temperature regime, these measurements confirm the overdamped behavior, since $\omega_0\tau\ll1$. Furthermore, all the parameters of CDW dynamics: ω_0, τ, and m^* are obtained by examining the full frequency range.

At temperatures below about 130 K, Figs. 4(b) and 5(b) show that because of the increased pinning frequency, it is no longer possible to treat the inertial and relaxational responses separately, as was possible at higher temperatures. Thus we have found it necessary to use Eq. (2), representing the full response of the CDW. However, now it is necessary to treat both $\sigma_{\max}$ and ω_0 as additional fit parameters, and a best fit is shown in Figs. 4(b) and 5(b). Again all the parameters: τ, ω_0, and m^* (from $\sigma_{\max}$ and τ) are obtained, by examining data only in the microwave and millimeter-wave spectral range.

At temperatures below about 60 K, the frequency dependence is much more complicated than the simple single oscillator descriptions used above [Fig. 4(c)], and a fit in terms of Eq. (2) is not possible. This is demonstrated in Fig. 4(c) where the measured $\mathrm{Re}\sigma_{\mathrm{CDW}}(\omega)$ is compared to Eq. (2). Consequently, we have not attempted to extract the parameters which characterize Eq. (2) for this temperature region. (For further discussions of the validity of the single oscillator description, see Sec. III C.)

The present work yields all the phenomenological parameters, τ, m^*, ω_0, and $\sigma_{\max}$, relevant to the single oscillator description of CDW dynamics. In the following we discuss the experimental findings and compare with available microscopic theories.

A. Damping (τ) and maximum conductivity ($\sigma_{\max}$)

The damping frequency $1/2\pi\tau$ determined at different temperatures in the CDW state is displayed versus temperature in Fig. 6(a). The remarkable feature of the results is that $1/2\pi\tau$ is relatively temperature independent between 100 and 210 K, increasing slightly near T_P.

In the temperature range 210 K to approximately 120 K (see Fig. 7), $\sigma_{\max}\simeq\sigma_n$, the conductivity in the normal state above T_P, since $\sigma_n=ne^2\tau_0/m_0$, where τ_0 is the

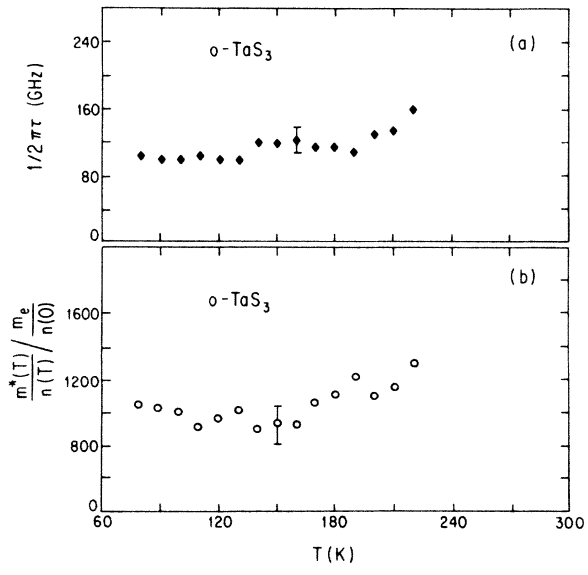

FIG. 6. (a) Damping frequency $1/2\pi\tau$ versus temperature T. (b) $m^*(T)/n(T)$ normalized to $m_e/n(0)$ versus temperature T.

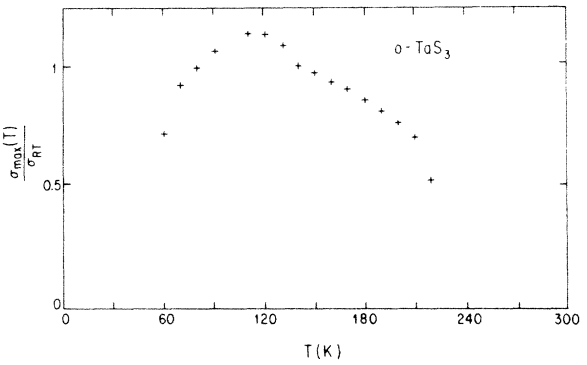

FIG. 7. Maximum conductivity $\sigma_{\max}(T)/\sigma_{RT}$ versus temperature.

damping time of normal electrons and m_0 is the band mass above T_P. This result implies $\tau/m^* \simeq \tau_0/m_0$, consistent with arguments[11] implying such a relationship. Hence the damping frequency $1/2\pi\tau$ in the CDW state is smaller by the factor m_0/m^* ($\simeq 10^3$) than the corresponding quantity $1/2\pi\tau_0$ in the normal state. This is why we are able to observe the Drude response of the CDW [Eq. (1)] in the mm-wave frequency range, in contrast to most metals, where the Drude response occurs at optical frequencies.

A microscopic theory of CDW damping has been initiated by Takada, Wong, and Holstein.[12] According to these authors, the dominant contribution arises from scattering with thermally ambient phasons. The effects of thermally generated acoustic phonons and amplitons are much weaker. Damping due to impurities and normal electrons is neglected. The results of the theory can be represented as

$$\frac{1}{2\pi\tau} = \frac{2^{1/2}}{2\pi}\left[\frac{\pi^4}{64}\right]\left[\frac{\lambda^2}{\mu\Omega_t}\right]T^2 , \tag{5}$$

where λ is the electron-phonon coupling constant, $\mu = m^*/m_b$, with m_b the band mass, and $\Omega_t = \omega_{2k_F}/2$. Since m_b is not known, we take $\mu = m^*/m_e$, available from the present measurements. The above result also leads to

$$\sigma_{\max} = \frac{ne^2\tau}{m^*} = \left[\frac{ne^2}{m_e}\right]\frac{64}{\pi^4\sqrt{2}}\left[\frac{\Omega_t}{\lambda^2}\right]\frac{1}{T^2} . \tag{6}$$

These expressions are valid well below T_P where $n(T) = n(T=0)$, since effects of quasiparticles are ignored. Thus in its present form, the theory predicts a T^2 dependence for $1/2\pi\tau$ and $1/\sigma_{\max}$ at low temperatures where the quasiparticle number is negligible. The above expressions are valid for $T > \Theta_D$, the Debye temperature, which is approximately 50 K for TaS_3. For $T < \Theta_D$, the theory predicts an even stronger temperature dependence, $1/\tau \propto T^5$.

The T^2 dependence for $1/2\pi\tau$ is not observed in the present experiment [see Fig. 6(a)] and the damping constant is nearly independent of temperature. Regarding magnitudes, using $\lambda = 0.34$, $\Omega_t = 25$ K, and $\mu = 940$, the theory yields $1/2\pi\tau = 4.6$ GHz at $T = 160$ K, nearly a factor of 24 lower than the experimental results.

The maximum conductivity $\sigma_{\max}$ does increase quite rapidly below T_P, in qualitative agreement with the predicted $1/T^2$ dependence. However, it must be remembered that in this region quasiparticle damping probably cannot be ignored. The theory yields $\sigma_{\max} = 6.3\times 10^4$ $(\Omega\,\mathrm{cm})^{-1}$ at 160 K, higher by 24 than the experimental value $\sigma_{\max} = 2.6\times 10^3$ $(\Omega\,\mathrm{cm})^{-1}$. At $T \lesssim 100$ K, $\sigma_{\max}$ begins to decrease. We associate this with the increasing disorder, possibly arising from increasing commensurability.

It would appear that the theory in its present form *underestimates* the magnitude of CDW damping. Further analysis by the same authors[13] indicates that Coulomb interactions, originally ignored, play an important role, and could significantly enhance the damping.

B. Effective mass (m^*)

From the experimentally determined τ and $\sigma_{\max} = ne^2\tau/m^*$, the effective mass m^* was determined. Strictly speaking, the experiments yield $m^*(T)/n(T)$, and this quantity normalized to the free-electron value $m_e/n(0)$ is plotted as a function of temperature in Fig. 6(b). At low temperature, since $n(T) = n(0)$, Fig. 6(b) directly yields m^*/m_e, which is seen to be $\sim 10^3$. The dynamical response of the CDW is thus characterized by a very high effective mass in o-TaS_3. Also, $m^*(T)/n(T)$ is nearly independent of T, except near T_P where it tends to increase slightly.

In mean-field theory the effective mass is given by[14]

$$\frac{m^*}{m_b} = 1 + \frac{4\Delta^2(0)}{\lambda\omega_{2k_F}^2}\frac{n(T)}{n(T=0)} . \tag{7}$$

Therefore mean-field theory predicts $m^*(T)/n(T)$ should be temperature independent since $m^*(T) \propto n(T) \propto \Delta^2(T)$. As is evident from Fig. 6(b), our results are in general agreement with this prediction except near T_P. Comparison between theory and experiment regarding magnitudes is dependent on parameter values in Eq. (7) for λ, ω_{2k_F}, and $\Delta(0)$. For TaS_3, it is reasonable to take $\lambda = 0.34$ and $\omega_{2k_F} = 50$ K, the same values as for $NbSe_3$. Using a mean-field result, $\Delta(0)/k_B = 1.74T_P = 390$ K yields $m^*/m_b \sim 715$. However, in TaS_3, due to strong one-dimensional fluctuations, $\Delta(0)$ can be considerably higher. From dc resistivity measurements below the Peierls transition, $\Delta(0) = 700$ K, which gives $m^*/m_b = 2200$. The experimental results lie between these two estimates, and considering the uncertainty in m_b, the agreement within a factor 2 is quite acceptable. The temperature dependence suggests that the mean-field theory is less appropriate near T_P. Overall our results indicate that while a mean-field theory is appropriate to a first approximation, additional effects may have to be included.

C. Pinned mode and oscillator strengths

The full frequency dependence of the CDW conductivity from 10^7 to 10^{11} Hz, including lower-frequency data, is

shown in Fig. 8 for both the real and imaginary parts. It is clear that in this range, the full response of the $q=0$ CDW phason mode is observed, which has a damped resonant character due to pinning, damping, and finite mass.

The solid line represents a fit to Eq. (2) based on a single oscillator model with parameters $\omega_0=5$ GHz, $1/2\pi\tau=125$ Ghz, and $\sigma_{\max}=\mathrm{Re}\sigma_{\mathrm{CDW}}(9\ \mathrm{GHz})$. While this simple oscillator description works well for the high-frequency part describing damping and inertia (as is to be expected from the discussion in Sec. III), the lower-frequency part disagrees (which had been known previously[8]). In this relaxational regime it is common to consider a distribution $P(\omega_0)$ of pinning frequencies. Such a description yields the dashed line in Fig. 8, from

$$\sigma_{\mathrm{CDW}}(\omega)=\int_0^\infty P(\omega_0)\sigma_{\mathrm{so}}(\omega_0)d\omega_0\ , \tag{8}$$

where σ_{so} is the single oscillator conductivity, given by Eq. (2). For Fig. 8, $P(\omega_0)=1$ for $\omega_0\leq 5$ GHz, $P(\omega_0)=0$ for $\omega_0>5$ GHz. It is seen that the distributed oscillator model yields a better fit to the lower-frequency data, and hence to the overall response. As is to be expected, the distribution of pinning frequencies does not affect the inertial response since the latter occurs at much higher frequencies.

An important quantity that can be obtained from the present measurements is the oscillator strength of the CDW mode. For a single collective mode whose linear response is given by Eq. (2),

$$\int_0^\infty \mathrm{Re}\sigma_{\mathrm{CDW}}(\omega)\,d\omega=\frac{\pi e^2}{2}\left[\frac{n(T)}{m^*(T)}\right]. \tag{9}$$

The temperature dependence of the inverse of this quantity has already been plotted in Fig. 6(b). From Fig. 6(b) we see that the oscillator strength is almost temperature independent, decreasing slightly near T_P. (In a mean-field theory it should be constant for $T\leq T_P$.)

The CDW contribution represented by the above equation, is $\sim 10^{-3}$ of the total oscillator strength (i.e., including all frequencies $\omega\rightarrow\infty$). This is due to the large effective mass, which makes the Drude response accessible on this mm-wave frequency range. Further, this area should be "missing" from the optical part of the conductivity spectrum at frequencies $\omega>\Delta$.

While the area under $\mathrm{Re}\sigma_{\mathrm{CDW}}$ is relatively temperature independent, the whole spectrum shifts to higher frequencies, as is evident from Fig. 4, as the temperature is lowered below approximately 100 K. This can be associated with the tendency of the CDW to become increasingly disordered, thus developing higher-frequency components, as the temperature is lowered.

As we have already remarked before, the frequency-dependent response at low temperatures appears to be more complicated, and a description in terms of a Drude response is not possible. Various evidences, such as long-time relaxational phenomena and remanent polarization effects suggest that at these temperatures disorder plays an especially important role, and this has been called a "charge-density-wave glass."[15] It is anticipated, that the ω dependent response is characterized by an extremely broad distribution of pinning frequencies, with an upper cutoff beyond the millimeter-wave spectral range. The results presented in Fig. 4(c) are indicative of such behavior, but we have not yet attempted to analyze our experimental data in detail. The frequency-dependent response may be further complicated in this temperature region because of commensurability effects, leading to soliton excitations[16] of the collective mode. Experiments at higher frequencies are required to clarify this point.

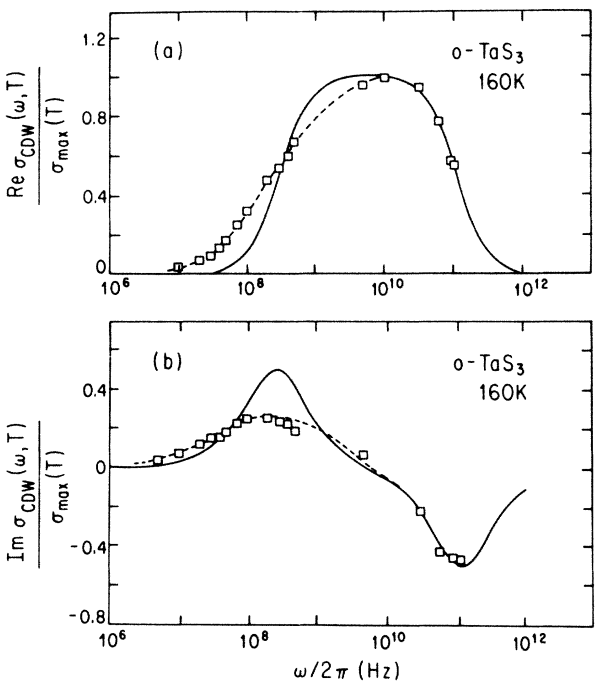

FIG. 8. CDW conductivity $\sigma_{\mathrm{CDW}}(\omega,T)$ normalized to $\sigma_{\max}(T)$ at $T=160$ K versus frequency $\omega/2\pi$, including the present higher-frequency data and other lower-frequency data (Refs. 5 and 7), thus covering the range 10^7–10^{11} Hz. (a) $\mathrm{Re}\sigma_{\mathrm{CDW}}(\omega,T)/\sigma_{\max}(T)$; (b) $\mathrm{Im}\sigma_{\mathrm{CDW}}(\omega,T)/\sigma_{\max}(T)$. The solid lines represent fits to the real and imaginary parts, respectively, of Eq. (2) with $\omega_0/2\pi=5$ GHz, $1/2\pi\tau=125$ GHz. The dashed line represents Eq. (7) with parameters discussed in the text. Above approximately 5 GHz the dashed and solid lines coincide.

IV. CONCLUSIONS

In this paper, and in I, we have presented clear evidence for inertia effects which characterize the dynamics of the collective mode in two, widely investigated model compounds, $NbSe_3$ and o-TaS_3. In both cases, the response in the microwave and millimeter-wave spectral range can be described by a Drude expression, and—with n evaluated from the known crystal structure and band filling—the parameters m^* and τ can be extracted. When combined with lower-frequency measurements, the pinning frequency ω_0 is also obtained. The magnitude and temperature dependence of the damping constant τ are, at present, not accounted for by theories and we conclude that damping associated with the dynamics of the pinned collective mode is not fully understood at present. Our results, together with those performed on alloys,[17] indicate that

TABLE I. Charge-density-wave parameters for $NbSe_3$ and TaS_3 deduced from the present experiments. N/A denotes not available.

	$NbSe_3$ (45 K)	$NbSe_3$ (120 K)	TaS_3 (160 K)	
Measured				
$\sigma_{max}=ne^2\tau/m^*$ $[(\Omega\,\mathrm{cm})^{-1}]$	24 000	2000	2500	
$1/2\pi\tau$ (sec^{-1})	70×10^9	90×10^9	125×10^9	
$\omega_{co}/2\pi=\omega_0^2\tau/2\pi$ (sec^{-1})	100×10^6	N/A	150×10^6	
$\omega_0/2\pi$ (sec^{-1})	2.6×10^9	N/A	4.3×10^9	
m^*/m_e	117,95[a]	270	940	
Calculated				
$\Delta(0)$ K	106[b]	253[b]	390[b]	700[c]
λ	0.32	0.30	0.34	
m^*/m_b	78	340	715	2303

[a] $m^*/m_e=95$ is deduced from a two-fluid model (see text).
[b] From mean-field theory, $\Delta(0)=1.74kT_p$.
[c] A. Zettl, G. Gruner, and A. H. Thompson, Phys. Rev. B **26**, 5760 (1982).

damping is not an impurity effect, but rather is determined by an intrinsic mechanism.

Well below the Peierls transitions, the measured effective masses are independent of the temperature, in agreement with the mean-field results, but increase when the Peierls transition is approached. This latter observation may be related to the effect of normal electrons, as discussed in I. In Table I, we have collected the measured effective-mass values at selected temperatures, in both phases of $NbSe_3$ and for o-TaS_3. The electron-phonon coupling constants [evaluated using the mean-field expression $\Delta=D\exp(-1/\lambda)$] are also given with our best estimates for the single-particle gap Δ. The mean-field expressions for m^*/m_e are also displayed in Table I. The agreement between our experimental values and the mean-field results is adequate, considering the uncertainties of the parameters involved. We also note that our results for m^*/m_b are different from those evaluated recently by Thorne *et al.*,[18] using the low-frequency end of the spectrum, and also the tunneling model.[19] The reason for the disagreement is not clear at present and the issue clearly requires further attention.

We have also examined the ω-dependent response in a broad frequency range, and analyzed the results in terms of a distribution of characteristic frequencies. Such a distribution does not affect the higher-frequency end of the spectral range, but leads to drastic deviations from a single harmonic oscillator response at radio frequencies. In this low-frequency regime, the tunneling model also gives an approximate description of the measured low-frequency response.[19]

Our results may also be related to the observed electric-field-dependent response, as various models suggest that the characteristic fields which describe $\sigma(E)$ are related to the characteristic pinning frequency ω_0. The relation between ω- and E-dependent response will be discussed in a later publication.

ACKNOWLEDGMENTS

We thank T. Holstein (deceased) and L. Mihaly for useful discussions, and B. A. Alavi and M. Maki for preparing samples. This work was supported in part by National Science Foundation Grants Nos. DMR-83-11843 and DMR-84-06896 and equipment contributions from Hughes Aircraft Co. and UCLA. One of us (D.R.) received financial support from IBM.

[1] K. Tsutsumi, K. Sambongi, S. Kagoshima, and T. Ishigura, J. Phys. Soc. Jpn. **44**, 1735 (1978).
[2] For a recent review, see G. Gruner and A. Zettl, Phys. Rep. **119**, 117 (1985).
[3] D. Reagor, S. Sridhar, and G. Gruner, preceding paper, Phys. Rev. B **34**, 2212 (1986).
[4] Z. Z. Wang, K. Salva, P. Monceau, M. Renard, C. Roncau, R. Aryoles, I. Levy, L. Guemas, and A. Meerschaut, J. Phys. (Paris) Lett. **44**, L311 (1983).
[5] S. Sridhar, D. Reagor, and G. Gruner, Phys. Rev. Lett. **55**, 1196 (1985).
[6] A. Zettl, C. M. Jackson, and G. Gruner, Phys. Rev. B **26**, 5773 (1982).
[7] J. H. Miller, J. Richard, J. R. Tucker, and John Bardeen, Phys. Rev. Lett. **51**, 1592 (1983).
[8] Wei-Yu Wu, L. Mihaly, G. Mozurkewich, and G. Gruner, Phys. Rev. Lett. **52**, 2382 (1982).
[9] S. Sridhar, D. Reagor, and G. Gruner, Rev. Sci. Instrum. **56**, 1946 (1985).
[10] G. Mihaly and L. Mihaly, Solid State Commun. **49**, 1009

(1984); G. Verma, N. P. Ong, S. K. Khanna, J. C. Eckert, and J. M. Savage, Phys. Rev. B **28**, 910 (1983).
[11]L. P. Gorkov and E. N. Doglov, J. Low Temp. Phys. **42**, 101 (1981); John Bardeen, Mol. Cryst. Liq. Cryst. **81**, 1 (1981).
[12]S. Takada, M. Wong, and T. Holstein, in *Charge Density Waves in Solids, Vol. 217 of Lecture Notes in Physics,* edited by Gy. Hutiray and J. Solyom (Springer-Verlag, Berlin, 1985), p. 227.
[13]T. Holstein (private communication).
[14]P. A. Lee, T. M. Rice, and P. W. Anderson, Solid State Commun. **14**, 703 (1974).
[15]A. Zettl, G. Gruner, and A. H. Thompson, Phys. Rev. B **26**, 5760 (1982).
[16]B. Horowitz and S. E. Trullinger, Solid State Commun. **49**, 195 (1985).
[17]D. Reagor and G. Gruner, Phys. Rev. Lett. **56**, 659 (1986).
[18]R. E. Thorne, J. H. Miller, W. G. Lyons, L. W. Lyding, and J. R. Tucker, Phys. Rev. Lett. **55**, 1006 (1985).
[19]John Bardeen, Phys. Rev. Lett. **51**, 1596 (1985), and references therein.